Modeling and Analysis

GREENHOUSE GASES SCIENCE AND TECHNOLOGY

Dynamic analysis of carbon dioxide desorption with 2-amino-2-methyl-1-propanol and piperazine blends

Armando Zanone, Mauá School of Engineering, Mauá Institute of Technology, Sao Caetano do Sul, SP, Brazil and Escola Politécnica of the University of São Paulo (USP), Sao Paulo, SP, Brazil
Wilson Miguel Salvagnini and José Luis de Paiva, Escola Politécnica of the University of São Paulo (USP), Sao Paulo, SP, Brazil

Abstract: In this study, the dynamic behavior of CO_2 desorption in an aqueous blend of 2-amino-2-methyl-1-propanol (AMP) and piperazine (PZ) was investigated. Solvent desorption, an important method used to capture CO_2 by absorption into amines, was carried out in a laboratory column with a film promoter and monitored online by infrared spectroscopy. A PLS model was used to quantify the free amines, carbonated species, and total absorbed CO_2 in all its chemical forms present in the liquid phase. The desorption was performed at atmospheric pressure and temperatures of 323, 333, and 343 K with blend solutions of 30/0, 25/5, 20/10, and 0/15 wt.% AMP/PZ. The liquid mass transfer coefficient (k_L) decreased with higher CO_2 loadings and was not significantly affected by temperature. AMP enhanced the liquid mass transfer coefficient of the PZ solvents, and the highest k_L occurred at the higher PZ blend concentrations. © 2021 Society of Chemical Industry and John Wiley & Sons, Ltd.

Additional supporting information may be found online in the Supporting Information section at the end of the article.

Keywords: amine blend; carbon capture; desorption; infrared; mass transfer

Introduction

Carbon dioxide (CO_2) is one of the main greenhouse gases due to its emissions on the larger scale. The primary sources of CO_2 emission arise from energy supply (47 %), industries (30%), transport (11%), and construction sectors (3%).[1] CO_2 has to be frequently removed or recovered from gaseous streams, either as a reagent, for example, synthesis gas, or as an impurity, since it reduces the specific heat of natural gas and becomes corrosive in water.[2,3]

CO_2 absorption using an aqueous amine solution is the most established, widely implemented method in the industry, and is considered the main process to reduce CO_2 emissions due to its higher absorption rate

Correspondence to: Armando Zanone, Mauá School of Engineering, Mauá Institute of Technology, Department of Chemical Engineering, Praça Maua, 1, CEP 09580–900, Sao Caetano do Sul, SP, Brazil.
Email: armando.zanone@maua.br
Received August 9, 2021; revised October 27, 2021; accepted October 28, 2021
Published online at Wiley Online Library (wileyonlinelibrary.com). DOI: 10.1002/ghg.2134

and efficiency in diluted gas streams compared to other technologies.[4–7] The drawback of this technology is the high energy consumption required to regenerate the solvent, which usually occurs at its boiling temperature. The energy required for the regeneration process may be as high as 75% of the total operating cost of a CO_2 capture plant, and the high temperature of the process could lead to problems such as amine vaporization, amine degradation, and device corrosion.[8–10]

Over the past decades, solvent blends have become of increasing interest to researchers, such as the mixture of 1-amino-2-methyl-1-propanol (AMP) and piperazine (PZ) which takes advantage of the high reaction rate of PZ with CO_2, as well as the high CO_2 loading capacity (α) and lower regeneration energy requirement of AMP. This blend has been studied and used in pilot-scale systems for amine-based CO_2 removal from flue gas.[1,11–22] This solvent blend has better performance in energy saving than the conventional monoethanolamine (MEA) solvent.[17,22] AMP at higher concentrations appears to catalyze the reaction of CO_2 and PZ by deprotonating it.[16] Furthermore, the HCO_3^- formed in the reaction of AMP and CO_2 increases amine deprotonation due to its lower pH compared to water and is easily desorbed. Moreover, both amines have low thermal degradability and are less corrosive than traditional amines.[11,23]

Usually, desorption is considered as the inverse process of absorption.[24] However, Kierzkowska-Pawlak and Chacuk[25] showed that absorption and desorption rates of a carbonated N-methyl-2-pyrrolidone in a batch system were different. Also, Jamal *et al.*[26] concluded that extrapolating the kinetic data of the absorption process led to different values of the experimental desorption rates. Thus, the desorption process should not be modeled as a simple inversion of the absorption process. Since in many practical situations, the operational and capital costs of the desorption column are higher than absorption costs, desorption studies are relatively scarce compared to the extensive work on absorption.[27] There are many investigations on the absorption kinetics in several alkanolamine solutions, but direct measurements of CO_2 desorption rates in aqueous amine solutions are limited.[28] Published desorption works usually study new solvents with a lower enthalpy of reaction.[6,16,19,25,28] They often evaluate controlled closed systems, such as reactors or wet wall columns, with slight variations in CO_2 concentration in the liquid phase, and generally at low temperatures (<340 K).

Chen *et al.*[29] have found that solutions of 5 M PZ absorb approximately 2.6 times faster than 7 M MEA and 1.3 times faster than 8 M PZ. Furthermore, they demonstrated that the advanced flash stripper reduced the energy requirement by 25%. Dugas and Rochelle[30] measured, using a wetted wall column, the mass transfer rates and coefficient of CO_2 in aqueous MEA and aqueous PZ from 313 to 373 K over a wide range of CO_2 loading for absorption and desorption processes. They found that the liquid phase mass transfer coefficient had almost no influence on temperature and amine concentration. Khan *et al.*[16] performed absorption experiments at nearly atmospheric pressure in a packed column with varying temperature, liquid flow rate, CO_2 partial pressure, and amine concentration. However, desorption was performed in a flask with a magnetic stirrer. They studied different PZ and AMP blends with a constant total amine concentration. Each mixture was reused five times (five cycles) for CO_2 capture with a vacuum stripping process. The regeneration efficiency decreased the most after the second cycle, and the efficiency was higher for higher AMP concentrations. Nonetheless, most researchers only studied the PZ monocarbamate formation and not the dicarbamate or protonated PZ ion.[17]

An accurate reactive mass transfer model is required to design and optimize the chemical desorption process.[31] Thus, it is necessary to quantify the chemical components present in both phases to understand the mechanisms of the process. Fourier transform infrared spectroscopy (FTIR) allows the identification and quantification of chemical compounds simultaneously in a fast and nondestructive way. In addition, this technique does not need sample preparation, such as dilution that may alter the chemical equilibria. Moreover, a multivariate regression method such as a PLS model significantly reduces the interference of compounds.[32–35]

In this study, online monitoring of the desorption process was used to investigate the solvent dynamic composition change, the flux rates, and mass transfer coefficients at three temperatures (323, 333, and 343 K), and four different amine blend compositions 30/0, 25/5, 20/10, and 0/15 wt.% AMP/wt.% PZ.

Materials and methods

Solutions

The reagents used were AMP (91±1 %, Sigma Aldrich), PZ (98±1 %, Sigma Aldrich), and distilled water. Samples weighing 500 g were prepared gravimetrically

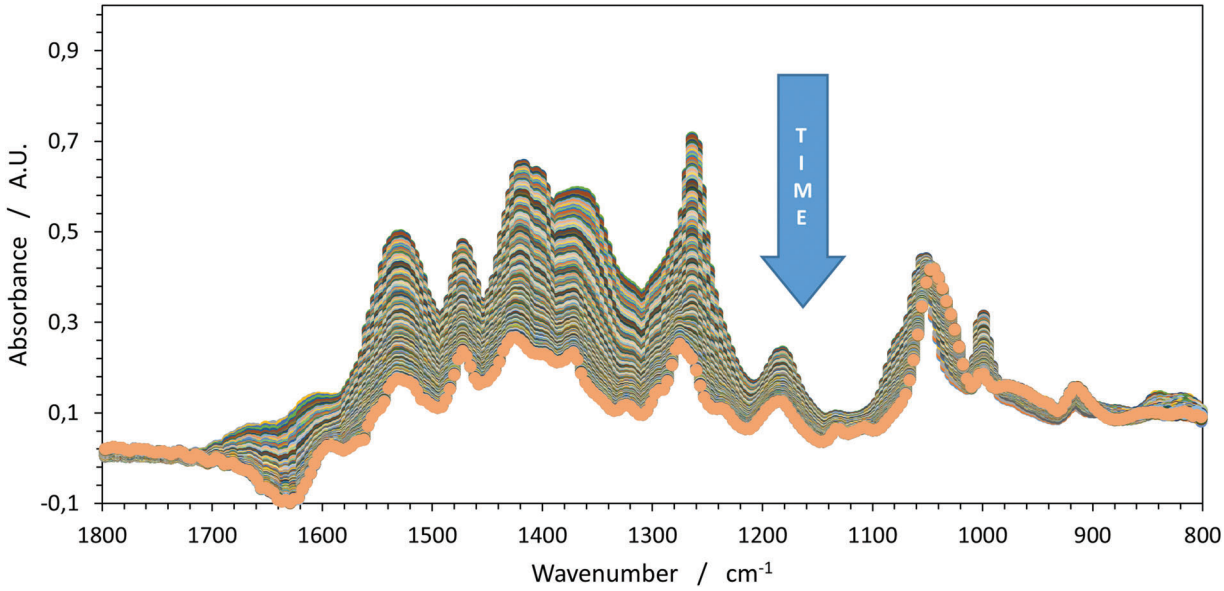

Figure 1. MIR spectra subtracted from the water spectrum for the 25/5 wt.%AMP/wt.%PZ desorption process at 333 K.

(analytical scale model AY220, Shimadzu). Each solution was bubbled with pure CO_2 (99.9 %, Air Liquide Brasil) until the infrared spectra remained constant and the sample was considered saturated (chemical equilibrium established). Although the actual CO_2 capture process could not reach equilibrium, part of the CO_2 would desorb during the preheating of the samples before experimenting. Four solutions were prepared for each investigated temperature: 30/0, 25/5, 20/10, and 0/15 wt.% AMP/wt.% PZ. Heating and mechanical stirring were needed to solubilize PZ in the highly concentrated solutions.

Concentration acquisition

The ReactIR 45m Fourier Transform Infrared (FTIR) spectrometer (Mettler-Toledo) with iC IR^{TM} v4.2.26 software collected all spectra data and simultaneously predicted the concentration of free AMP and PZ, bicarbonate, and PZ mono- and dicarbamate. Measurements were taken in the wavenumber range of 4000–650 cm^{-1} at a spectral resolution of 4 cm^{-1} with 32 scans. The equipment had a controller that maintained the liquid cell temperature at 303 K. Figure 1 shows the MIR spectra collected for one of the experiments, the 25/5 wt.%AMP/wt.%PZ at 333 K, representing the intermediate condition.

The concentration of the liquid phase was predicted using a Partial Least Square model (PLS) developed by Wold *et al.*[37] which is a common chemometrics method.[38,39] The PLS model explains the variation in the responses (concentration of the chemical component) and dependent predictors (IR spectra) by constructing latent variables or factors that directly relate to the source data.[33] The method will try to find the multidimensional direction in the predictor space that explains the maximum multidimensional variance direction in the response space using a linear model. The optimal number of factors is selected such that adding another factor does not improve the quality of the model.[40]

A PLS[42] model predicted the concentration of the liquid phase using the infrared spectra acquired online. The 1303–836 cm^{-1} region contained all the information used in all models. Table 1 summarizes the PLS specifications for each chemical species, the training coefficient of determination (R^2), the validation coefficient of determination (Q^2), the root-mean-square error of calibration (RMSEC), and the root-mean-square error of prediction (RMSEP). Every PLS model was validated using a leave-one-out cross validation algorithm and the quality was assessed via the RMSEP.[41] Details of the model can be found in our previous work.[42]

Desorption process

Figure 2 shows a flowchart of the desorption process. First, an electrical resistance was used (i) to boil water in a 5 L Erlenmeyer, which preheated (ii) atmospheric

Table 1. PLS specifications, coefficient of determination, and root-mean-square errors for each chemical species model.

Species concerned	Region (cm^{-1})	Pre-Treatment	Number of Factors	R^2	Q^2	RMSEC	RMSEP
AMP	1082-1026	9 points Savitz-Golay	10	0.999	0.997	0.127	1.540
PZ	1140-1080	9 points Savitz-Golay	7	0.999	0.994	0.180	0.652
$PZCOO^-$	1303-1250	second derivative	1	0.458	0.315	0.436	1.346
$^-OOCPZCOO^-$	1303-1250	none	1	0.904	0.811	0.826	1.553
HCO_3^-	845-836	second derivative	1	0.994	0.980	0.255	1.396
Total CO_2 absorbed	1690-846	none	8	0.999	0.994	0.019	0.223

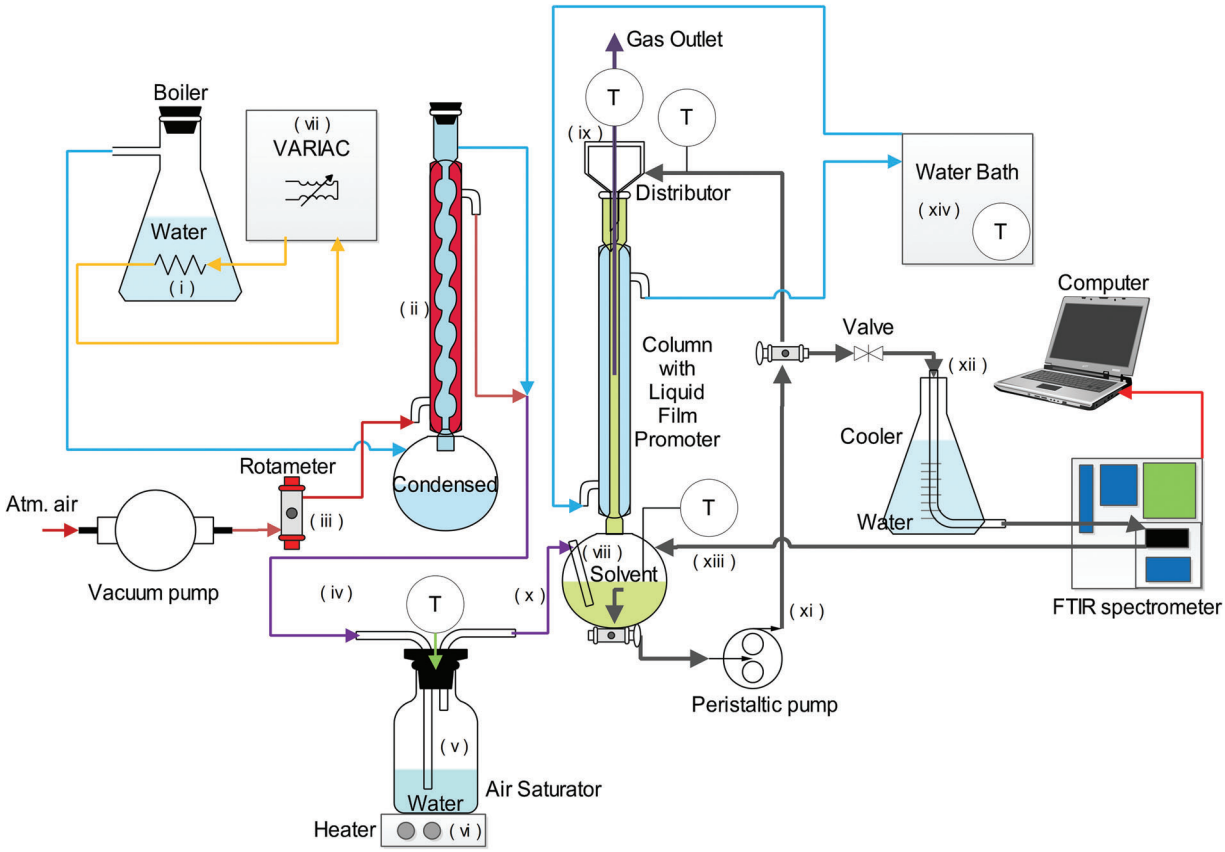

Figure 2. Desorption process flowsheet.

air at a constant flow rate of 100 mL·s^{-1} (iii). This steam mixed with the hot air (iv) bubbled into water in a heated 2 L flask (v), thus saturating it at the desired temperature. The heating plate power was used to control the temperature of the air saturator (vi). In addition, an electrical resistance (vii) was used to regulate the level of water inside the air saturation flask. A separate water bath heated the desorption sample solution. When the sample solution and saturated air reached the desired process temperature, the round flask (viii) was filled with the solvent through the top of the column (ix) to ensure that the entire wall-film promoter (Fig. 3) would wet. The saturated air (x) bubbled up into the solution (viii), allowing its homogenization. A constant flow rate of 3.5 mL·s^{-1} of solvent (xi) entered a distributor at the top of the column, which spread the liquid, wetting the entire perimeter of the promoter. About 0.3 mL·s^{-1} of the flow rate (xii) passed through water flask at room-temperature to cool the solution and not

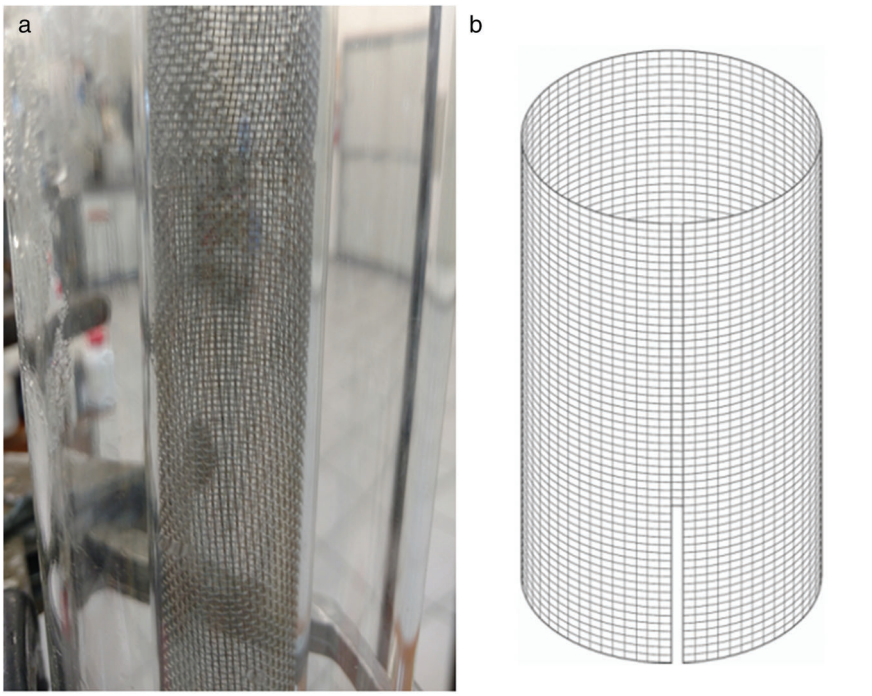

Figure 3. Stainless steel 28-mesh film promoter.

overload the spectrometer cooling system. The software collected spectra of the sample every 30 s, after it, which the solution returned to the flask (xiii). A water bath (xiv) controlled the temperature of the liquid film inside the column.

The column consisted of a 0.5 m long vertical cylinder with an inner diameter of 22 mm where the liquid flowed downward as a film on the wall, and the air flowed upward. A 28-mesh stainless steel woven wire film promoter covered the entire inner area of the column, which increased the interfacial area of mass and heat transfer. It also guarantees that the fluid scatters over the entire vertical surface of the column for low liquid flow rates, as already used in past work.[43] Figure 3A shows a picture of the promoter and Fig. 3B a representation of it. The column also had a concentric cylinder shell where water heated the liquid film. The distributor consisted of two concentric cylinders with a 1-mm space through which the solvent flowed. All silicon hoses were thermally isolated with polyethylene foam.

Altogether, 14 experiments were performed. Four concentrations of the solvent (30/0, 25/5, 20/10, 0/15 wt.% AMP/wt.% PZ) at three temperatures (323, 333, and 343 K) at local atmospheric pressure of 94 kPa. The intermediate condition of 25/5 wt.% AMP/wt.% PZ at 333 K was run in triplicate.

Desorption computations

The mass of the carbonated solutions before and after each desorption experiment was weighed. It was assumed that there was no entrainment of the amines or the carbonated products. Then, as the liquid composition was measured, a simple mass balance using Eqns (1) and (2) allowed calculation of the total mass of desorbed CO_2 could be calculated, as well as evaporated or condensed water. Also, Eqns (3) allowed the calculation of the molar flux of CO_2.

$$\frac{dM}{dt} = \dot{m}_{H_2O} + \dot{m}_{CO_2} \quad (1)$$

$$\frac{d\left(Mx_{CO_2}\right)}{dt} = \dot{m}_{CO_2} \quad (2)$$

$$N_{CO_{2,t}} = \frac{\dot{m}_{CO_2,t}}{A_{promoter}} \quad (3)$$

The loading represents the total molar quantity of CO_2 divided by the initial total amine molar quantity (AMP+PZ). The CO_2 concentration in the inlet gas (bottom of the column) was assumed to be zero, and the CO_2 partial pressure in the outlet (top of the column) was calculated by a mass balance.

The gas temperature was assumed to be equal to the temperature measured at the top of the column

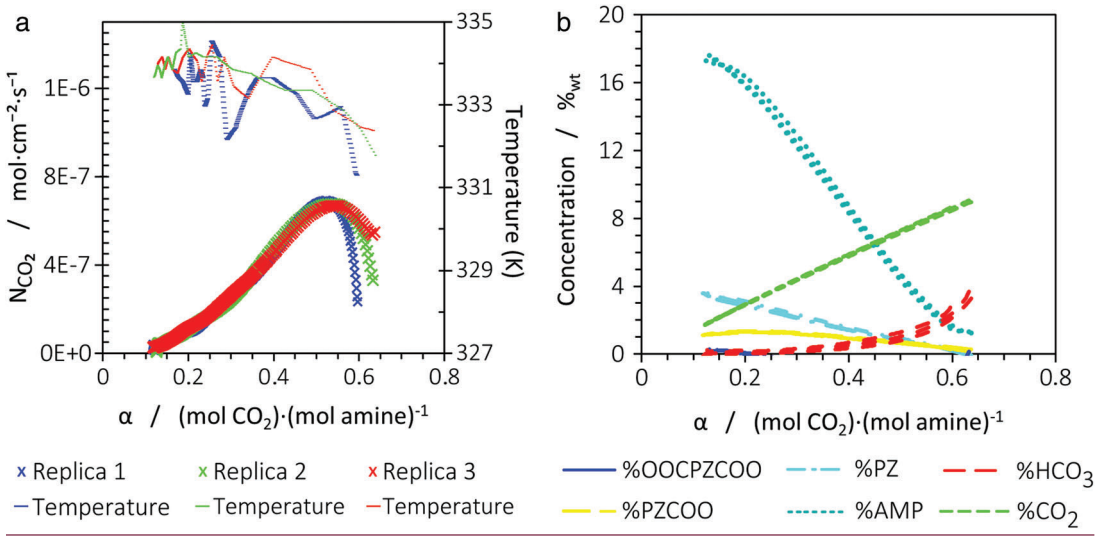

Figure 4. CO_2 flux rate and liquid phase concentration in triplicates.

(outlet). The measured water bath, liquid, and gas temperature allowed the calculation of the liquid film temperature using the heat transfer resistance through the glass wall and the film thickness.[44] Values reported in the literature were used for density,[45] viscosity,[45] and CO_2 solubility.[46–50]

The overall mass transfer coefficient (K_G) was calculated by the ratio of the desorption flux and the log mean CO_2 partial pressure driving force, as shown in Eqn (4), where $P^*_{CO_2,t}$ is the CO_2 pressure that would be in equilibrium at the given liquid loading with the AMP and PZ composition.

$$K_{G,t} = \frac{N_{CO_2,t}}{\left(\frac{-P_{CO_2,t}}{\ln\left(\frac{P^*_{CO_2,t}-P_{CO_2,t}}{P^*_{CO_2,t}}\right)}\right)} \quad (4)$$

The two-film model, Eqn. (5), was used to calculate the chemical liquid mass transfer coefficient (k_L) and a correlation[51] was used to determine the gas mass transfer coefficient (k_G).

$$\frac{1}{K_G} = \frac{1}{k_G} + \frac{1}{Ek_L} \quad (5)$$

Results and discussion

Reproducibility analysis

The desorption process at 333 K for the 25/5 wt.% AMP/wt.% PZ, which corresponds to an intermediate condition of temperature and concentration, was performed in triplicate. The mean difference between the weighed total mass of desorbed CO_2 and the calculated total mass of CO_2 desorbed using Eqns (1) and (2) was 4.5%. Figure 4A compares the CO_2 flux rate and Fig. 4B the liquid phase concentration for each replica. They are similar except at the beginning of the process at higher loadings, where there is a slight difference between the replicas, probably, due to the different start temperatures of each experiment. After a few minutes, all experiments reached the desired process temperature and had the same flux and mass transfer. Temperature variations of ±2 K in the liquid and ±5 K in the gas phase did not seem to affect N_{CO2} and k_L. The concentrations, Fig. 4B, could be considered equal, except for bicarbonate that had a small difference at higher loadings.

Data pretreatment

Instead of comparing the raw data, the following graphs and data were filtered to avoid misinterpretation. Data that represented operational errors were removed, such as those caused by air bubbles in the spectrometer leading to negative concentrations, and temperature variations above ±2 K due to lack of control. These filtered data appear as gaps in the graphs.

Composition

As the desorption rate is less intense at lower temperatures, in Fig. 5 the concentration for each blend composition was shown at 323 K. The concentration profile at higher temperatures is similar except for a lower initial loading since more CO_2 desorbs during the preheating. That also explains why

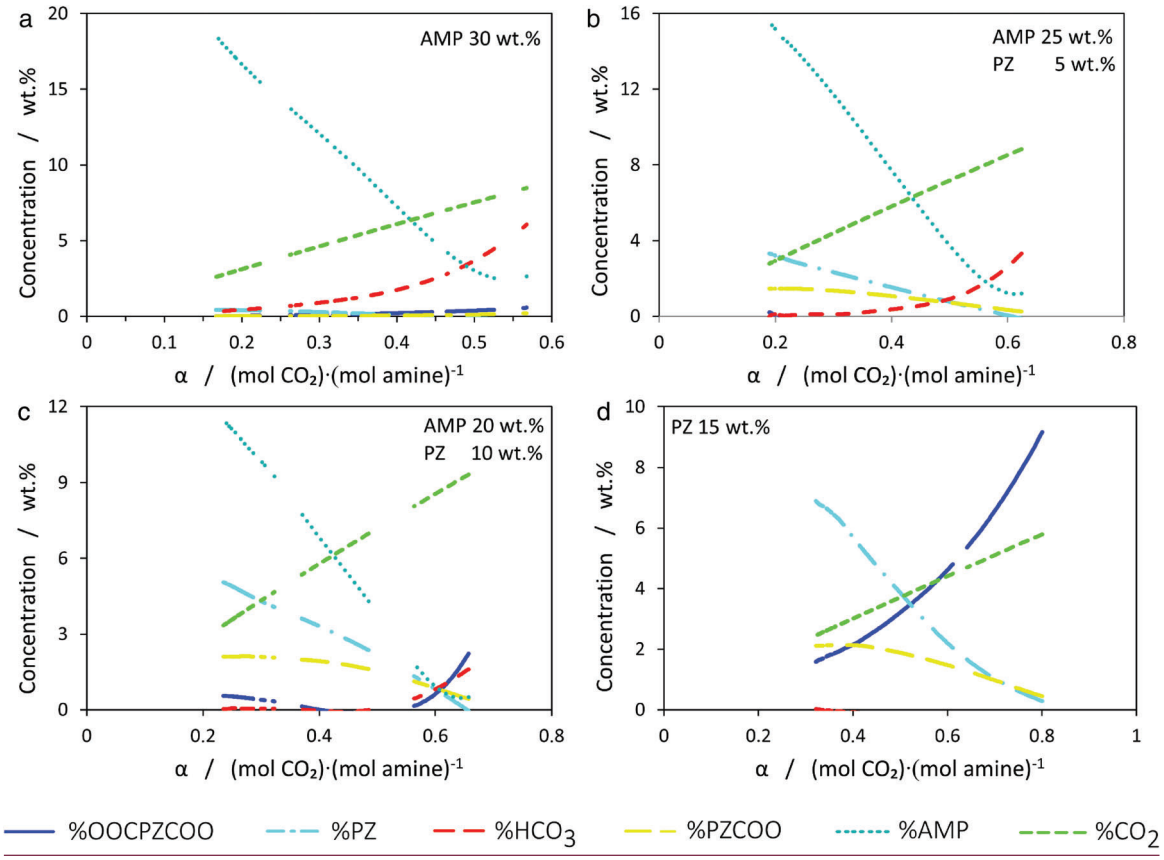

Figure 5. Mass concentration for different solvent composition at 323 K.

the concentration at high loadings is not seen. Thus, a wider range of loadings can be covered. Figure 5 shows the concentration of AMP, PZ, PZ monocarbamate ($PZCOO^-$), PZ dicarbamate ($^-OOCPZCOO^-$), bicarbonate (HCO_3^-), and total CO_2 absorbed. The latter one represents the sum of all carbamates and carbonates, even those not quantified, such as soluble CO_2. As expected, there is a linear correlation between CO_2 and the loading.

Figure 5 indicates synergy between AMP and PZ. Bicarbonate and PZ dicarbamate concentration rapidly decreases at loadings higher than 0.4. When the solvent contains only PZ, Fig. 5D, the dicarbamate PZ is always present in the solution, and for AMP, Fig. 5A, the bicarbonate tends to zero at loadings lower than 0.2. However, in the blends, there is no significant amount of bicarbonate and PZ dicarbamate at loadings lower than 0.3. As shown in Fig. 5B and Fig. 5C, only PZ monocarbamate had not desorbed. The remaining PZ monocarbamate could not be desorbed at the current temperature. Therefore, loadings lower than 0.2 could not be achieved.

CO_2 flux rate

Figure 6 shows the CO_2 flux rate for each solvent blend at (a) 323, (b) 333, and (c) 343 K.

The CO_2 flux rate increases at higher loadings regardless of the temperature and amine composition. The fluxes ranged from 10^{-8} to 10^{-6} mol·cm^{-2}·s^{-1}. The higher both the PZ concentration in the solvent and the loading, the higher the flux rate. Even a solvent with half of the total amine concentration, 15 wt.% PZ, showed a higher flux rate than the AMP blends. At lower loadings, the higher the AMP concentration in the solvent, the higher the CO_2 flux rate. Moreover, we can infer that higher temperatures increase CO_2 flux rates.

Liquid mass transfer coefficient

Figure 7 shows the chemical mass transport coefficients of the liquid phase for each solvent composition at (a) 323, (b) 333, and (c) 343 K. The 20/10 and most of the 25/5 wt.% AMP/wt.% PZ data at 343 K are not shown due to temperature variations higher than 2 K. We

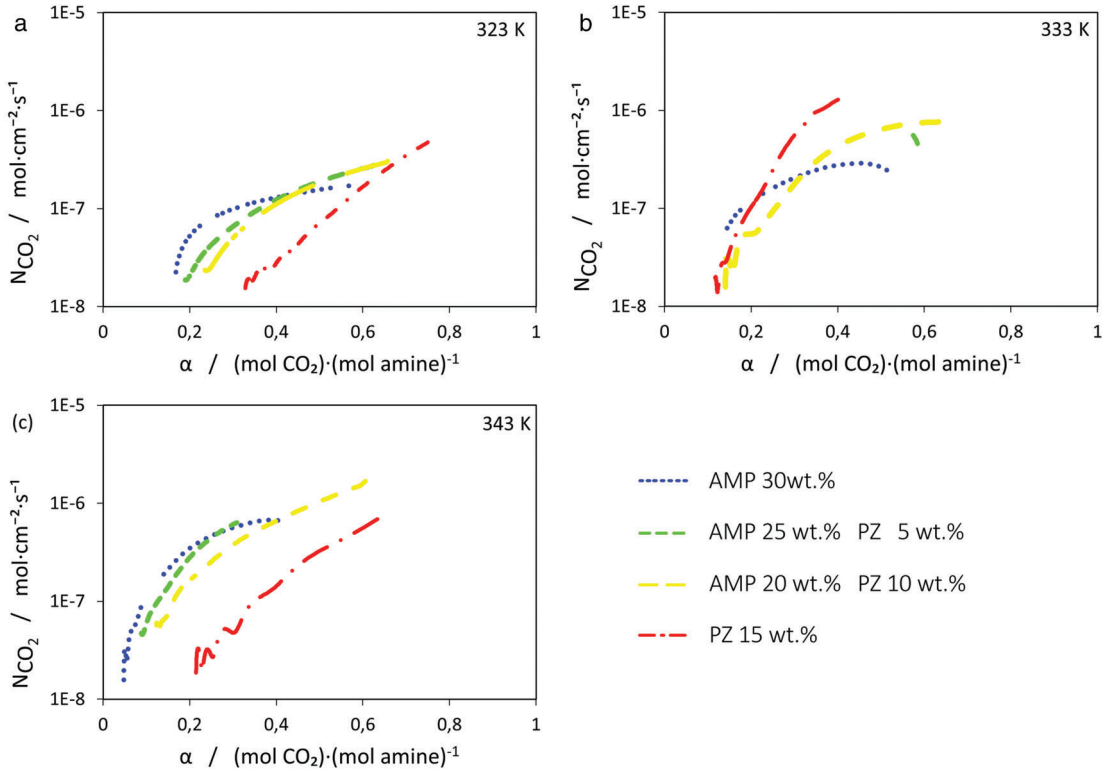

Figure 6. CO_2 flux at different liquid temperatures for different solvent compositions.

could not determine k_L at loadings below 0.25 as we would need to extrapolate the CO_2 partial pressure at equilibrium reported in the literature.[49,50]

The PZ solvent showed a nearly linear correlation between k_L and the loading, whereas k_L rapidly increased for low loadings in the AMP solutions.

There is an evident synergy between AMP and PZ at all temperatures. Both single amine solvents had lower k_L values than the blend solutions. Although the pure PZ solution had the lowest values of k_L, the blend with a higher PZ concentration had the highest k_L value. One possible explanation is that the single PZ carbonated solution had half of the AMP concentration, 15 and 30 wt.%, respectively. The synergy occurs by faster zwitterion deprotonation of PZ (Eqn 6) due to the higher basicity of AMP compared to water, increasing the k_L for the blend compared to the single amine solvents, also suggested by Khan *et al.*[16]

$$H^+PZCOO^- + AMP \rightleftharpoons AMPH^+ + PZCOO^- \quad (6)$$

There was no significant effect of the temperature on k_L. Therefore, the loading and the amine concentration are the main factors of influence. The mass transfer coefficients behavior agreed with literature results.[30]

Figures 6 and 7 show an oscillation in the flux rates and k_L that occurs at loadings lower than 0.2 due to a slow desorption rate, so the changes in CO_2 concentration are equal, in order of magnitude, as the PLS model uncertainty.

Conclusions

Real-time predictions of the concentrations of nonreacted AMP and PZ, PZ mono and dicarbamate, and bicarbonate could be made using FTIR spectroscopy. Also, the prediction of the total CO_2 absorbed in the liquid phase allowed the determination of its flux rate and the chemical liquid mass transfer coefficient (k_L). The PZ solvent had the lowest k_L, followed by the AMP solvent, while the blend had a higher k_L for higher PZ concentrations. Results showed that AMP enhanced the reaction of PZ with CO_2 compared to water. Moreover, k_L increased at lower loadings and was not significantly affected by temperature in the 323–343 K range.

Symbols

A [m^2]	area
E	enhance factor

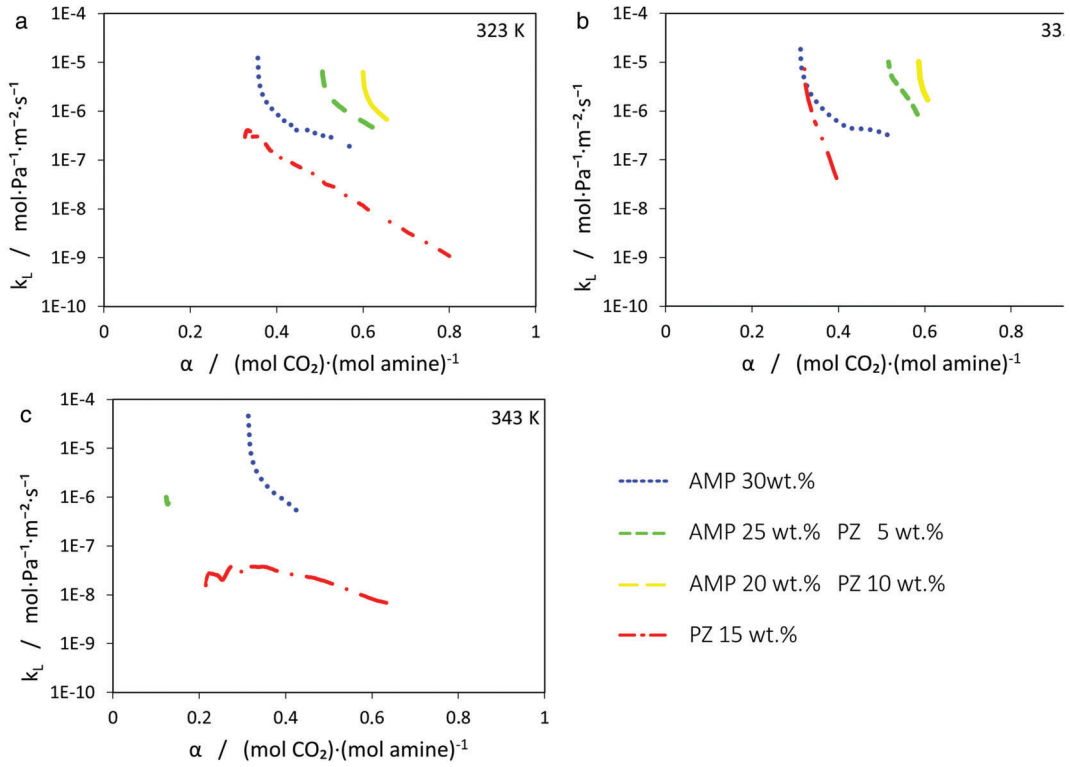

Figure 7. Individual liquid mass transfer coefficient for each blend at different loadings.

k [mol·Pa^{-1}·m^{-2}·s^{-1}]	individual mass transfer coefficient
K [mol·Pa^{-1}·m^{-2}·s^{-1}]	overall mass transfer coefficient
$\dot{m}$ [kg·s^{-1}]	mass flow rate
M [kg]	mass
N [mol·cm^{-2}·s^{-1}]	molar flux rate
P [Pa]	partial pressure
T [K]	temperature
X	mass fraction

Greek letters

α	carbon dioxide loading (mol of CO_2 per mol of amine)

Acknowledgements

This work was supported by the CNPq Brazil (Conselho Nacional de Desenvolvimento Científico e Tecnológico) and CAPES (Coordenação de Aperfeiçoamento de Pessoal de Nível Superior).

Conflict of Interest

The authors declare no conflict of interest.

References

1. Khan AA, Halder GN, Saha AK. Carbon dioxide capture characteristics from flue gas using aqueous 2-amino-2-methyl-1-propanol (AMP) and monoethanolamine (MEA) solutions in packed bed absorption and regeneration columns. Int J Greenhouse Gas Control. 2015;32:15–23. https://doi.org/10.1016/j.ijggc.2014.10.009
2. Datta AK, Sen PK. Optimization of membrane unit for removing carbon dioxide from natural gas. Membr Sci. 2006;283(1–2):291–300. https://doi.org/10.1016/j.memsci.2006.06.043
3. Saghafi H, Arabloo M. Modeling of CO_2 solubility in MEA, DEA, TEA, and MDEA aqueous solutions using AdaBoost-decision tree and artificial neural network. Int J Greenhouse Gas Control. 2017;58:256–65. https://doi.org/10.1016/j.ijggc.2016.12.014
4. Jackson P, Robinson K, Puxty G, Attalla M. In situ Fourier transform-infrared (FT-IR) analysis of carbon dioxide absorption and desorption in amine solutions. Energy Procedia. 2009;1(1):985–94. https://doi.org/10.1016/j.egypro.2009.01.131
5. Rochelle GT. Amine scrubbing for CO_2 capture. Science. 2009;325(5948):1652–4. https://doi.org/10.1126/science.1176731
6. Nwaoha C, Saiwan C, Supap T, Idem R, Tontiwachwuthikul P, Rongwong W, *et al*. Carbon dioxide (CO_2) capture performance of aqueous tri-solvent blends containing 2-amino-2-methyl-1-propanol (AMP) and methyldiethanolamine (MDEA) promoted by diethylenetriamine (DETA). Int J Greenhouse Gas Control. 2016;53:292–304. https://doi.org/10.1016/j.ijggc.2016.08.012

7. Wen L, Liu H, Rongwong W, Liang Z, Fu K, Idem R, *et al*. Comparison of overall gas-phase mass transfer coefficient for CO_2 absorption between tertiary amines in a randomly packed column. Chem Eng Technol. 2015;38(8):1435–43. https://doi.org/10.1002/ceat.201400606
8. Aaron D, Tsouris C. Separation of CO_2 from flue gas: a review. Sep Sci Technol. 2005;40(1–3):321–48. https://doi.org/10.1081/SS-200042244
9. Idem R, Wilson M, Tontiwachwuthikul P, Chakma A, Veawab A, Aroonwilas A, *et al*. Pilot plant studies of the CO_2 capture performance of aqueous MEA and mixed MEA/MDEA solvents at the university of regina CO_2 capture technology development plant and the boundary dam CO_2 capture demonstration plant. Ind Eng Chem Res. 2006;45(8):2414–20. https://doi.org/10.1021/ie050569e
10. Mores P, Scenna N, Mussati S. CO_2 capture using monoethanolamine (MEA) aqueous solution: Modeling and optimization of the solvent regeneration and CO_2 desorption process. Energy. 2012;45:1042–58. https://doi.org/10.1016/j.energy.2012.06.038
11. Dash SK, Bandyopadhyay SS. Carbon dioxide capture: absorption of carbon dioxide in piperazine activated concentrated aqueous 2-Amino-2-Methyl-1-Propanol. J Clean Energy Technol. 2013;1(3):184–8. https://doi.org/10.7763/jocet.2013.V1.42
12. Li H, Li L, Nguyen T, Rochelle GT, Chen J. Characterization of piperazine/2-aminomethylpropanol for carbon dioxide capture. Energy Procedia. 2013;37:340–52. https://doi.org/10.1016/j.egypro.2013.05.120
13. Li H, Frailie PT, Rochelle GT, Chen J. Thermodynamic modeling of piperazine/2-aminomethylpropanol/CO_2/water. Chem Eng Sci. 2014;117:331–41. https://doi.org/10.1016/j.ces.2014.06.026
14. Li H, Moullec YL, Lu J, Chen J, Marcos JCV, Chen G, *et al*. CO_2 solubility measurement and thermodynamic modeling for 1-methylpiperazine/water/CO_2. Fluid Phase Equilib. 2015;394:118–28. https://doi.org/10.1016/j.fluid.2015.03.021
15. Hairul NAH, Shariff AM, Tay WH, Mortel AMAVD, Lau KK, Tan LS. Modelling of high pressure CO_2 absorption using PZ+AMP blended solution in a packed absorption column. Sep Purif Technol. 2016;165:179–89. https://doi.org/10.1016/j.seppur.2016.04.002
16. Khan AA, Halder GN, Saha AK. Experimental investigation of sorption characteristics of capturing carbon dioxide into piperazine activated aqueous 2-amino-2-methyl-1-propanol solution in a packed column. Int J Greenhouse Gas Control. 2016;44:217–26. https://doi.org/10.1016/j.ijggc.2015.11.020
17. van der Spek M, Arendsen R, Ramirez A, Faaij A. Model development and process simulation of postcombustion carbon capture technology with aqueous AMP/PZ solvent. Int J Greenh Gas Control. 2016;47:176–99. https://doi.org/10.1016/j.ijggc.2016.01.021
18. Krótki A, Tatarczuk A, Stec M, Spietz T, Więcław-Solny L, Wilk A, *et al*. Experimental results of split flow process using AMP/PZ solution for post-combustion CO_2 capture. Greenhouse Gases: Sci Technol. 2017;7:550–61. https://doi.org/10.1002/ghg.1663
19. Nwaoha C, Idem R, Supap T, Saiwan C, Tontiwachwuthikul P, Rongwong W, *et al*. Heat duty, heat of absorption, sensible heat and heat of vaporization of 2–amino–2–methyl–1–propanol (AMP), piperazine (PZ) and monoethanolamine (MEA) tri–solvent blend for carbon dioxide (CO_2) capture. Chem Eng Sci. 2017;170:26–35. https://doi.org/10.1016/j.ces.2017.03.025
20. Osagie E, Biliyok C, Di Lorenzo G, Manovic V. Process modelling and simulation of degradation of 2-amino-2-methyl1-propanol (AMP) capture plant. Energy Procedia. 2017;114:1930–9. https://doi.org/10.1016/j.egypro.2017.03.1324
21. Wang T, He H, Yu W, Sharif Z, Fang M. Process simulations of CO_2 desorption in the interaction between the novel direct steam stripping process and solvents. Energy Fuels 2017;31(4):4255–62. https://doi.org/10.1021/acs.energyfuels.7b00009
22. Zhang W, Chen J, Luo X, Wang M. Modelling and process analysis of post-combustion carbon capture with the blend of 2-amino-2-methyl-1-propanol and piperazine. Int J Greenhouse Gas Control. 2017;63:37–46. https://doi.org/10.1016/j.ijggc.2017.04.018
23. Namjoshi O, Hatchell D, Rochelle GT. Thermal degradation of PZ-activated tertiary and hindered amines. 12th International Conference Greenhouse Gas Technologies, Austin, Texas. October; 2014.
24. Danckwerts PV. Gas – liquid reactions. New York: McGraw Hill Book Co; 1970.
25. Kierzkowska-Pawlak H, Chacuk A. Carbon dioxide desorption from saturated organic solvents. Chem Eng Technol. 2010;33(1):74–81. https://doi.org/10.1002/ceat.200900334
26. Jamal A, Meisen A, Lim JC. Kinetics of carbon dioxide absorption and desorption in aqueous alkanolamine solutions using a novel hemispherical contactor—II: experimental results and parameter estimation. Chem. Eng Sci. 2006;61(19):6590–603. https://doi.org/10.1016/j.ces.2006.04.047
27. Tunnat A, Behr P, Görner K. Desorption kinetics of CO_2 from water and aqueous amine solutions. Energy Procedia. 2013;51:197–206. https://doi.org/10.1016/j.egypro.2014.07.023
28. Kierzkowska-Pawlak H, Chacuk A. Kinetics of CO_2 desorption from aqueous N-methyldiethanolamine solutions. Chem Eng J. 2011;168(1):367–75. https://doi.org/10.1016/j.cej.2011.01.039
29. Chen E, Zhang Y, Lin Y, Nielsenb P, Rochelle G. Review of recent pilot plant activities with concentrated piperazine. Energy Procedia. 2017;114:1110–1127. https://doi.org/10.1016/j.egypro.2017.03.1266
30. Dugas RE, Rochelle GT. Modeling CO_2 absorption into concentrated aqueous monoethanolamine and piperazine. Chem Eng Sci. 2011;66(21):5212–8. https://doi.org/10.1016/j.ces.2011.07.011
31. Diab F, Provost E, Laloué N, Alix P, Souchon V, Delpoux O, *et al*. Quantitative analysis of the liquid phase by FT-IR spectroscopy in the system CO_2/diethanolamine (DEA)/H_2O. Fluid Phase Equilib 2012;325:90–99. https://doi.org/10.1016/j.fluid.2012.04.016
32. Einbu A, Ciftja AF, Grimstvedt A, Zakeri A, Svendsen HF. Online analysis of amine concentration and CO_2 loading in MEA solutions by ATR-FTIR spectroscopy. Energy Procedia 2012;23:55–63. https://doi.org/10.1016/j.egypro.2012.06.040
33. Kachko A, van Der Ham LV, Geers LFG, Huizinga A, Rieder A, Abu-Zahra MRM, *et al*. Real-time process monitoring of CO_2 capture by aqueous AMP-PZ using chemometrics: pilot plant demonstration. Ind Eng Chem Res 2015;54(21):5769–76. https://doi.org/10.1021/acs.iecr.5b00691

34. Kachko A, van Der Ham LV, Bardow A, Vlugt TJH, Goetheer ELV. Comparison of Raman, NIR, and ATR FTIR spectroscopy as analytical tools for in-line monitoring of CO_2 concentration in an amine gas treating process. Int J Greenhouse Gas Control. 2016;47:17–24. https://doi.org/10.1016/j.ijggc.2016.01.020
35. van der Ham LV, Bakker DE, Geers LFG, Goetheer ELV. Inline monitoring of CO_2 absorption processes using simple analytical techniques and multivariate modeling. Chem Eng Technol. 2014;37(2):221–8. https://doi.org/10.1002/ceat.201300249
36. Martens H, Naes T. Multivariate calibration. Chichester, UK: John Wiley & Sons; 1993.
37. Wold S, Ruhe A, Wold H, Dunn III WJ. The collinearity problem in linear regression. The partial least Squares (PLS) approach to generalized inverses. SIAM J Scl Stat Comput. 1984;5(3):735–43. https://doi.org/10.1137/0905052
38. Fülöp A, Hancsók J. Comparison of calibration models based on near-infrared spectroscopy data for the determination of plant oil properties. Hung J Ind Chem. 2009;37(2):119–22. https://doi.org/10.3303/cet0917075
39. Wold S, Sjöström M, Eriksson L. PLS regression: a basic tool of chemometrics. Chemom Intell Lab Syst. 2001;58:109–130. https://doi.org/10.1016/S0169-7439(01)001551
40. Wise BM, Gallagher NB, Bro R, Shaver JM, Windig W, Scott-Koch R. PLS Toolbox 3.5 for use with MATLAB. Manson, WA: Eigenvector Research Inc; 2005.
41. Refaeilzadeh P, Tang L, Liu H. Cross-validation. In: Liu L, Özsu MT, editors. Encyclopedia of database systems. New York: Springer; 2009. p. 532–538. http://dblp.uni-trier.de/db/reference/db/c.html#RefaeilzadehTL09
42. Zanone A, Tavares DT, Paiva JL. An FTIR spectroscopic study and quantification of 2-amino-2-methyl-1-propanol, piperazine and absorbed carbon dioxide in concentrated aqueous solutions. Vib Spectrosc. 2018;99:156–61. https://doi.org/10.1016/j.vibspec.2018.03.007
43. Salvagnini WM, Taqueda MES. A falling-film evaporator with film promoters. Ind Eng Chem Res. 2004;43(21):6832–5. https://doi.org/10.1021/ie0307636
44. Spedding PL. Thermopedia. 2010. [cited7 September 2018] Available from: http://www.thermopedia.com/content/19/ https://doi.org/10.1615/AtoZ.f.falling_film_flow
45. Samanta A, Bandyopadhyay SS. Density and viscosity of aqueous solutions of piperazine and (2-amino-2-methyl-1-propanol + piperazine) from 298 to 333 K. J Chem Eng. Data 2006;51(2):467–70. https://doi.org/10.1021/je050378i
46. Aroua BMK and Salleh RM. Solubility of CO_2 in aqueous piperazine and its modeling using the Kent-Eisenberg approach. Chem Eng Technol. 2004;27(1):65–70. https://doi.org/10.1002/ceat.200401852
47. Safdar R, Thanabalan M, Omar AA. Solubility of CO_2 in 20 Wt. % aqueous solution of piperazine. Procedia Eng. 2016;148:1377–9. https://doi.org/10.1016/j.proeng.2016.06.607
48. Tong D, Maitland GC, Trusler MJP, Fennell PS. Solubility of carbon dioxide in aqueous blends of 2-amino-2-methyl-1-propanol and piperazine. Chem Eng Sci. 2013;101:851–64. https://doi.org/10.1016/J.CES.2013.05.034
49. Tontiwachwuthikul P, Melsen A, Lim CJ. Solubility of carbon dioxide in 2-amino-2-methyl-1-propanol solutions. J Chem Eng Data. 1991;36(1):130–3. https://doi.org/10.1021/je00001a038
50. Yang ZY, Soriano AN, Caparanga AR, Li MH, Equilibrium solubility of carbon dioxide in (2-amino-2-methyl-1-propanol + piperazine + water). J Chem Thermodyn. 2010;42(5):659–65. https://doi.org/10.1016/j.jct.2009.12.006
51. Hines AL, Maddox RN. Mass transfer: fundamentals and applications. New Jersey: Prentice Hall; 1985.

Armando Zanone

Armando Zanone is a doctoral student from Department of Chemical Engineering, Polythechnic School of the University of São Paulo. He received his BSc degree from the Department of Chemical Engineering, Mauá Engineering School, in 2015, MSc degree from Department of Chemical Engineering, EPUSP in 2017. His research interest is in environmental issues.

Wilson Miguel Salvagnini

Wilson Miguel Salvagnini is an assistant professor at the Chemical Engineering Department of the Polythechnic School of the University of São Paulo, where he received his BSc, MSc and PhD degrees in 1974, 1979 and 1989. His research interests include the development of separation process.

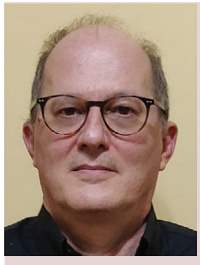

José Luis de Paiva

José Luis de Paiva is an assistant professor at the Chemical Engineering Department of the Polythechnic School of the University of São Paulo, where he received his BSc, MSc and PhD degrees in 1985, 1993 and 1999. His scientific interests include the development of mass transfer operations and multiphase processes.

